Dynamic Behaviour of a Wind Energy Conversion System Including Doubly-Fed Induction Generator in Fault Conditions

Dimitrios G. Giaourakis* , Athanasios Safacas* , Savvas Tsotoulidis*

*Laboratory of Electromechanical Energy Conversion, Department of Electrical Engineering and Computer Science, University of Patras

‡ Corresponding Author; Dimitrios G. Giaourakis,University of Patras, Rio-Patras 26504, +302610996894, dgkiaourakis@ece.upatras.gr, a.n.safacas@ece.upatras.gr, stsotoulidis@ece.upatras.gr

Received: 31.01.2012 Accepted:03.04.2012

Abstract- In this paper, the behaviour of a wind energy conversion system that uses the structure of Doubly-Fed Induction Generator (DFIG) under faulty conditions is presented. DFIG consists of an asynchronous machine, in which the stator is connected directly to the grid and its rotor is connected to the grid via two electronic power converters (back-to-back converter). In the three-phase rectifier and the inverter with IGBTs the Pulse Width Modulation (PWM) and SPWM technique is respectively used. DFIG is analysed and simulated under faulty conditions in the environment of Matlab/Simulink. The faults that are investigated in this work take place in the part of the back-to-back converter (either in the rectifier or in the inverter). More specifically, it is investigated how DFIG reacts when an open circuit happens in two IGBTs of the rectifier or of the inverter. Also, the results of Fourier analysis of some important system variables in these faulty conditions are presented and an identification of these faults is done.

Keywords- DFIG, simulation, back-to-back converter, PWM, faults.

1. Introduction

Various types of systems for wind potential conversion have been designed and are in operation. Each one of them has advantages and disadvantages and they could be used in specific occasions. The most important of these systems are presented in [4].

In this work the behaviour of a wind energy conversion system with Doubly-Fed Induction Generator (DFIG) is studied. This type of system has some advantages. One of them is that it can be operated in the region of low wind speeds e.g. 4m/s. The variable speed range of such wind energy systems is about 30% below and above the synchronous speed. The rating of the used back-to-back power converter is 25-35% of the generator capacity [5, 6], which made this an economical choice compared to the full power converter design of most other variable speed wind turbines. For these systems monitoring and diagnosis are important to prevent faulty conditions that maybe have negative consequences. Fault diagnosis could be achieved by measuring some characteristic quantities of the system in healthy condition, registering data and comparing them with the corresponding ones in the faulty condition, which prevails for a time after the fault beginning. So, fault diagnosis and identification could be achieved.

As it is documented in the international literature, the faulty conditions that have been investigated mostly are faults in the asynchronous generator (i.e unbalanced stator conditions, a broken bar), in the grid side such as voltage sags and in the DC link such as DC link fluctuation [7,8].

In this work faults in the back-to-back converter are studied, when the DFIG operates in subsynchronous mode, so the Grid Side Converter (GSC) operates as a boost rectifier without using the upper IGBTs, but only the corresponding diodes (Fig. 1). Two types of defects can appear on IGBT-an open circuit or a short circuit fault. These faults can appear in one IGBT only or in two IGBTs either in the same leg of the converter, or in two different legs. Open-circuit faults in two IGBTs in RSC or in GSC in different legs are investigated here.

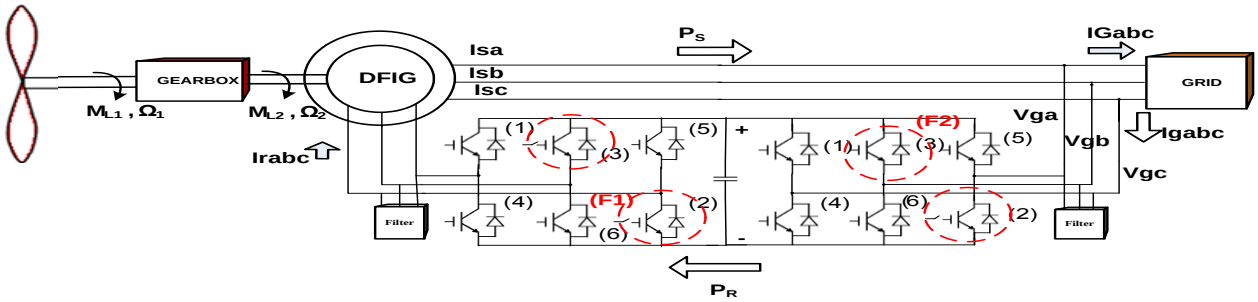

Fig. 1. Block diagram of DFIG.

2. A Brief Description of the Wind Energy Conversion System Including DFIG

2.1. General Aspects

The system's structure including DFIG (Fig.1) consists of an asynchronous machine that operates in generation mode, of which the stator is connected directly to the grid of constant voltage and frequency and the rotor plugging in the grid via a back-to-back power electronic converter. This system is used to achieve a wide range of operation modes from subsynchronous to supersynchro-nous (positive and negative slip). This can be achieved via power flow in both directions. That is why the bi-directional topology of AC/DC/AC converter is more preferable. Moreover, a back-to-back converter, being compared with most of the configurations with cycloconverters, line-commutated converters and low-frequency forced commutated thyristor converters, has a lot of advantages such as reduced harmonic distortion, higher power factor and control flexibility. The rotor electrical power P_r is only a fraction of stator output active power P_s (P_r=-sP_s). Since the electromagnetic torque Mel is negative in case of power generation and Ω_s is positive and constant for a constant frequency grid voltage, the sign of P_r depends on the slip (s) sign. For supersynchronous speed operation P_r is transmitted to DC bus capacitor and tends to raise the DC voltage. For subsynchronous speed operation P_r is taken out of the DC bus capacitor C and tends to decrease the DC bus voltage.

2.2. Wind Turbine Model

It is well-known that the relation between the wind speed and aerodynamic power is described by the following equation:

$$P_W = \frac{1}{2}\rho A C_p(\lambda,\beta) v_w^3 \tag{1}$$

and the corresponding torque is expressed as

$$T_w = \frac{1}{2}\rho\pi R^3 v_w^2 \frac{C_p(\lambda,\beta)}{\lambda} \tag{2}$$

where P_w is the aerodynamic power extracted from the wind [W], T_w is the corresponding aerodynamic torque [Nm], ρ the air density [kg/m^3], R the wind turbine rotor radius [m], v_w the equivalent wind speed [m/s], β the pitch angle of rotor [deg], C_p the power coefficient with its maximum value at 0.59 (Betz limit) and λ is the tip speed ratio given by the following equation:

$$\lambda = \frac{\omega_{wt} R}{v_w} \tag{3}$$

where ω_{wt} is the wind turbine rotor speed [rad/s].

2.3. DFIG Mathematical Model

This system is used to achieve a wide range of operation modes from subsynchronous to super-synchronous operation, namely the generator to operate with positive and negative slip. This can be achieved if the power converter can operate with power flow in both directions. [9,10]

The analysis and simulation of the DFIG operation is based on the well-known dynamical model described by the following equations (synchronously frame):

$$\left.\begin{aligned} u_{Sd} &= R_S \cdot i_{Sd} - \omega_s \Psi_{Sq} + \frac{d\Psi_{Sd}}{dt} \\ u_{Sq} &= R_S \cdot i_{Sd} + \omega_s \Psi_{Sd} + \frac{d\Psi_{Sq}}{dt} \end{aligned}\right\} \tag{4}$$

$$\left.\begin{aligned} u_{Rd} &= R_S \cdot i_{Rd} + \frac{d\Psi_{Rd}}{dt} - (\omega_s - \omega_R)\Psi_{Rq} \\ u_{Rq} &= R_S \cdot i_{Rq} + \frac{d\Psi_{Rq}}{dt} + (\omega_s - \omega_R)\Psi_{Rd} \end{aligned}\right\} \tag{5}$$

$$\left.\begin{aligned} \Psi_{Sd} &= (L_{S\sigma} + L_m) i_{Sd} + L_m i_{Rd} \\ \Psi_{Sq} &= (L_{S\sigma} + L_m) i_{Sq} + L_m i_{Rq} \end{aligned}\right\} \tag{6}$$

$$\left.\begin{aligned} \Psi_{Rd} &= (L_{R\sigma} + L_m) i_{Rd} + L_m i_{Sd} \\ \Psi_{Rq} &= (L_{R\sigma} + L_m) i_{Rq} + L_m i_{Sq} \end{aligned}\right\} \tag{7}$$

where u_{Sd}, u_{Sq}, u_{Rd} , u_{Rq}, i_{Sd}, i_{Sq}, i_{Rd}, i_{Rq}, Ψ_{Sd} , Ψ_{Sq} , Ψ_{Rd} , Ψ_{Rq} are voltages [V], currents [A] and flux linkages [Wb] of the stator and rotor in d- and q-axis, R_S is the resistance of the stator windings [Ω], L_S, L_R, L_m, are the stator, rotor and mutual inductances [H], $L_{R\sigma}$, $L_{S\sigma}$ the stator and rotor leakage inductances [H] and ω_s , ω_R are the angular frequency of the stator and rotor.

By calculating the apparent power and taking the real parts, the following equations represent the stator-side and rotor-side active and reactive power respectively:

$$\left.\begin{aligned} P_S &= \tfrac{3}{2}\left(u_{Sd}i_{Sd} + u_{Sq}i_{Sq}\right) \\ P_R &= \tfrac{3}{2}\left(u_{Rd}i_{Rd} + u_{Rq}i_{Rq}\right) \end{aligned}\right\} \quad (8)$$

$$\left.\begin{aligned} Q_S &= \tfrac{3}{2}\left(u_{Sq}i_{Sd} - u_{Sd}i_{Sq}\right) \\ Q_R &= \tfrac{3}{2}\left(u_{Rq}i_{Rd} - u_{Rd}i_{Rq}\right) \end{aligned}\right\} \quad (9)$$

The electromagnetic torque is expressed as:

$$M_{el} = p(i_q\Psi_{Sd} - i_d\Psi_{Sq}) \quad (10)$$

where p is the number of pole pairs.

Equation (11) describes the torque balance in DFIG:

$$(J_M + J_L)\frac{d\Omega}{dt} + M_{el} = M_L, \quad (11)$$

where M_L is the mechanical torque produced by wind turbine, *Mel* the electromagnetic torque of the asynchronous generator, J_M the moment of inertia of the asynchronous machine and J_L the moment of inertia of the wind turbine (and other mechanical parts).

3. Power Electronic Conversion System Control

3.1. Rotor Side Converter (RSC)

Rotor side converter acts as a PWM rectifier during the machine working in supersynchronous mode and as an inverter during subsynchronous mode. The purpose of the rotor side converter's control is the independent control of the rotor's active and reactive power. To succeed it, the voltages and the currents are transformed in d-, q-synchronously reference frame, where the d-axis is aligned with the air gap's flux vector. This happens because the stator of the DFIG is directly connected to the grid's voltage. This means that Ψ_S is constant and Ψ_{Sq} is equal to zero. So the following relations are applied:

$$\Psi_S = \Psi_{Sd} = const,\ \frac{d\Psi_{Sd}}{dt} = 0,\ \Psi_{Sq} = 0\ ,\frac{d\Psi_{Sq}}{dt} = 0 \quad (12)$$

Neglecting the small stator's resistance R_s , the voltage u_{Sd}=0 and the following current equations solving (6) are obtained:

$$i_{Sq} = -\frac{L_m}{(L_{S\sigma}+L_m)}i_{Rq},\ \ i_{Sd} = \frac{\Psi_{Sa}-L_m i_{Rd}}{(L_{S\sigma}+L_m)} \quad (13)$$

By substituting these equations to (7)-(11), the active and reactive power are given by the following equations:

$$P_s = -\frac{3}{2}u_{Sq}\frac{L_m}{(L_{S\sigma}+L_m)}i_{Rq},\ Q_s = \frac{3}{2}u_{Sq}\frac{\Psi_{Sd}-L_m I_{Rd}}{(L_{S\sigma}+L_m)} \quad (14)$$

From the equations (14), it is concluded that independent control of active and reactive power can be succeeded. Finally, the electromagnetic torque is given by the following equation:

$$M_{el} = -\frac{3}{2}\left(\frac{p}{2}\right)\Psi_{dq}\frac{L_m}{(L_{S\sigma}+L_m)}i_{Rq} \quad (15)$$

3.2. Grid Side Converter (GSC)

The grid side converter acts as a PWM inverter during the machine working in supersynchronous mode and as a rectifier during subsynchronous mode. In subsynchronous mode, the rotor's power is coming from the capacitor of the DC link, so the voltage interconnection is dropped down. This leads to power transportation from the grid to the capacitor. In supersynchronous mode the rotor feeds the capacitor, its voltage increases and the grid side converter transfers active power to the grid. Moreover, the reactive power that is exchanged between grid side converter and the grid, can be controlled. In our case the upper IGBTs of the GSC are always off, while the corresponding parallel diodes conduct.

The control of this converter is achieved by transforming the three phase quantities to d-, q- synchronously frame, in which the d-axis is aligned with the vector of the grid's voltage, because grid's voltage is constant. So, the following relations are resulted:

$$u_{gd} = u_d = const, \frac{du_{gd}}{dt} = 0, u_{gq} = 0, \frac{du_{gq}}{dt} = 0 \quad (17)$$

where u_{gd} is the component of grid voltage in d-axis and u_{gq} is the component of grid voltage in q-axis.

Through the following equations the active and reactive power can be calculated:

$$P_{gc} = \tfrac{3}{2}u_{gd}i_{gd}\ ,\ \ Q_{gc} = -\tfrac{3}{2}u_{gd}i_{gq} \quad (18)$$

These equations show that independent active and reactive power control can be achieved.

4. Faults Study in DFIG

A lot of fault types can appear within an electromechanical system. Some of them are [9, 10, 11]: (a) input supply single line to ground, (b) rectifier diode short or open-circuit fault, (c) dc link capacitor short-circuit fault, (d) dc link short-circuit to ground, (e) IGBTs short or open-circuit fault, (f) line to line short-circuit at machine terminal, (g) single line to ground fault at machine, (h) current sensors faults, (i) faults in induction motor (i.e. broken bar).

In DFIG the types of faults usually appear are a), f), g) and i) [12, 13,14]. In this work faults in the converters are studied (e). More specifically, open circuit in two IGBTs is investigated.

In Figure 1 the location of two faults (F1, F2) is chosen. In case of (F1), if the upper switch T3 of phase (b) and the lower switch T2 of the phase (c) are simultaneously opened, the defect causes a loss of reversibility in currents of two faulty switches. Thus, the two currents of the two faulty arms became unidirectional and nonsinusoidal. The loss of an alternation for each faulty phase, will involve a deformation on the third current, and since the neutral is insulated, this is almost null when the two currents of phases are simultaneously null. A typical example for the switching operation of the RSC in healthy and faulty condition can be seen in Fig. 2 (three signals). The time interval is specific and chosen around 90° of the voltage reference sinus

waveform for PWM. It can be seen that in faulty condition less current flows through T4 , T5 and D6, while D5 doesn't conduct.

Similarly, the switching operation of the GSC in healthy and faulty condition is shown in Fig. 3. In case of (F2), since T2 has an open-circuit fault (F2), only its diode (D2) is conducting in specific time intervals. Furthermore, a decrease of the currents flow through diodes D1, D2 and an increase of the diode D6 current can be observed.

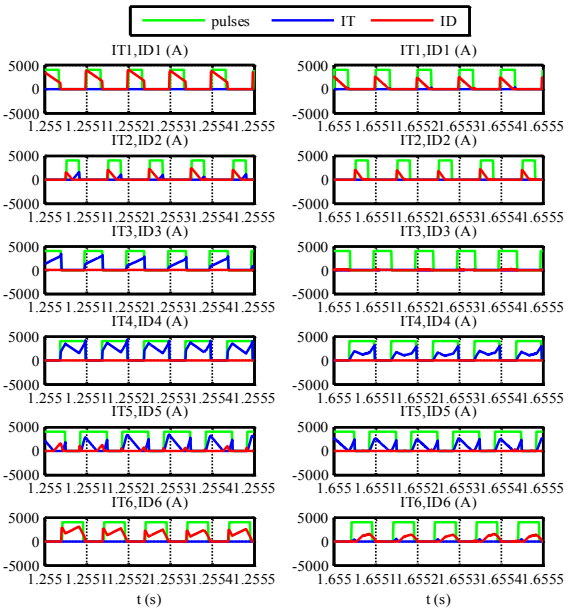

(a) (b)

Fig. 2. Switching operation of RSC (turn on pulses and currents) in (a) healthy condition and (b) faulty condition, ID=diode current, IT=IGBT current.

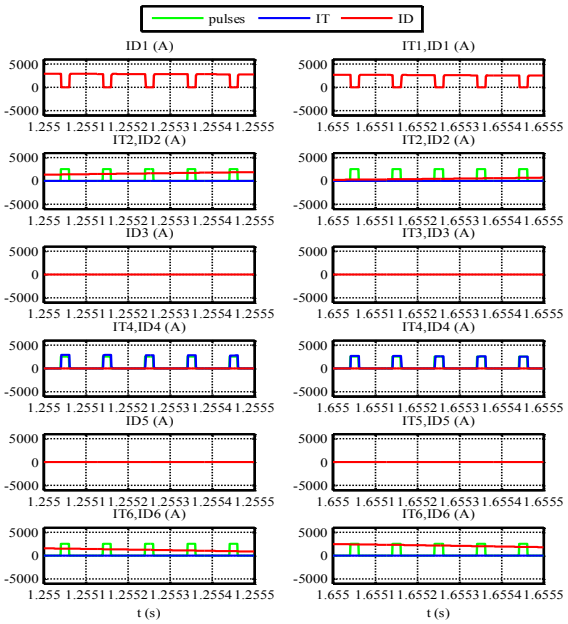

(a) (b)

Fig. 3. Switching operation of GSC (turn on pulses and currents) in (a) healthy condition and (b) faulty condition, ID=diode current, IT=IGBT current.

5. Investigation of DFIG System BehaviourThrough Simulation

5.1. DFIG Parameters

To study in detail the behaviour of a 1.5 MW DFIG, when the open-circuit faults, that have been described before, happen, the whole system has been simulated in Matlab/Simulink environment and some characteristic results are presented in each case of fault. Furthermore, FFT analysis for fault diagnosis and identification has been held. In this study a constant value of wind speed is considered. So, the wind turbine and rotor speed of the asynchronous machine is specific and equal to 1200 *rpm* (DFIG operates in subynchronous mode). Parameter values for the asynchronous machine are presented in Table 1.

Table 1. Parameter values of DFIG

P_N (MW)	V_N (V)	p	R_S (Ω)	L_{lS} (H)	R_R (Ω)	L_{lR} (H)	L_m (H)
1.5	690	2	0.01	0.003	0.02	0.003	0.03

In the rotor side converter SPWM modulation technique with f_{sw}=10 *kHz* and in the grid side converter PWM modulation technique with variable duty cycle is used. Parameters' value of filters: a) rotor side converter: C_r=*50mF*, L_r=*1μH,* b) grid side converter: C_g=*6mF*, L_g=*0.25mH.* The value of the C_{DClink} is equal to *30mF*. These values have been empirically chosen.

5.2. Open-Circuit Faults in RSC

The reaction of DFIG in this fault is presented through the waveforms of voltages, currents and electromagnetic torque shown in Fig.4-11. In Fig.4, 5 V_{gabc} voltages and the currents that are fed in the back-to back converter from the grid (I_{gabc}) are shown. It is concluded that this kind of fault (F1) hasn't any influence in this part of the whole system.

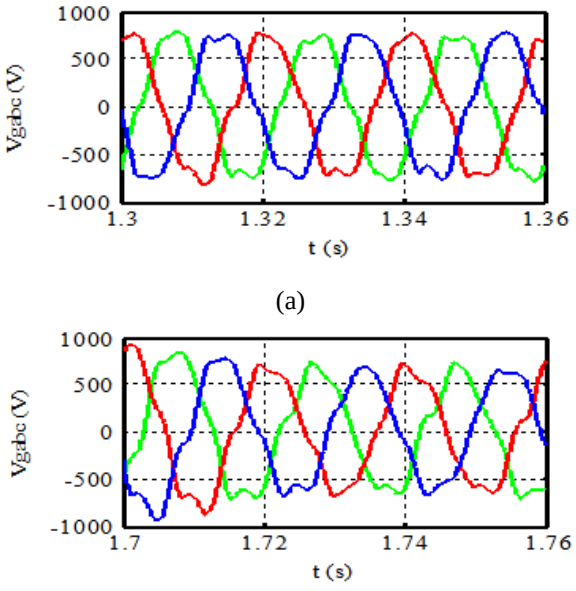

(a)

(b)

Fig. 4. Waveform of V_{gabc} voltages (a) in healthy and (b) in faulty condition.

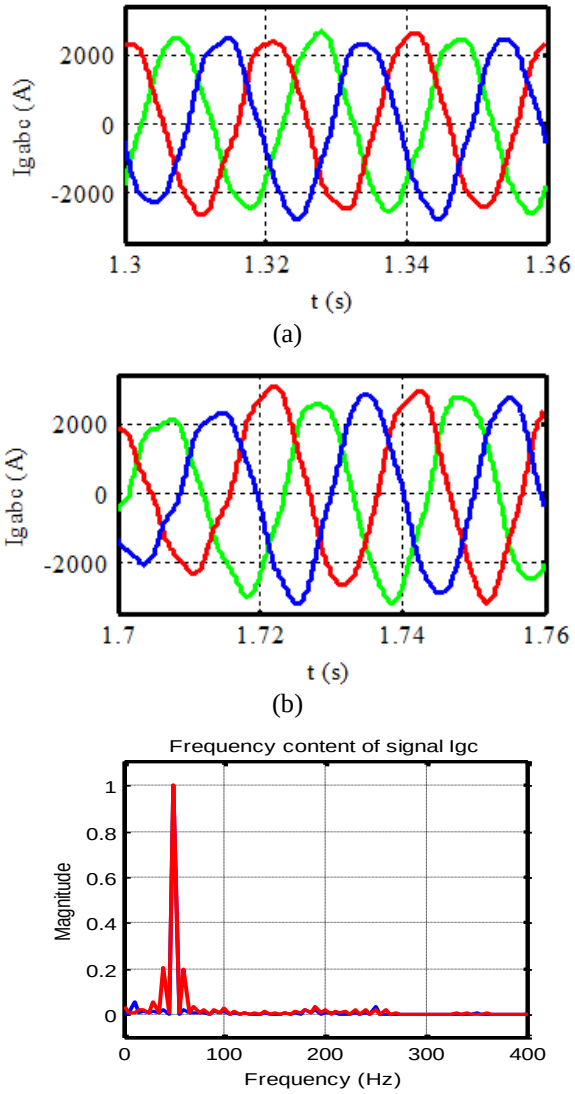

Fig. 5. Waveform of I_{gabc} currents (a) in healthy, (b) in faulty condition and (c) the spectrum of the current waveform of I_{gc} (blue line-healthy condition, red line-faulty condition).

In Figure 6 the waveforms of grid phase current (currents that are fed in the grid) are presented. It is upcoming that a high distaurbunce will occur beacause of the corresponding distrurbance of the stator's phase currents that fed in the grid. Also, in Fig. 7 the disturbance of DC link voltage could be seen.

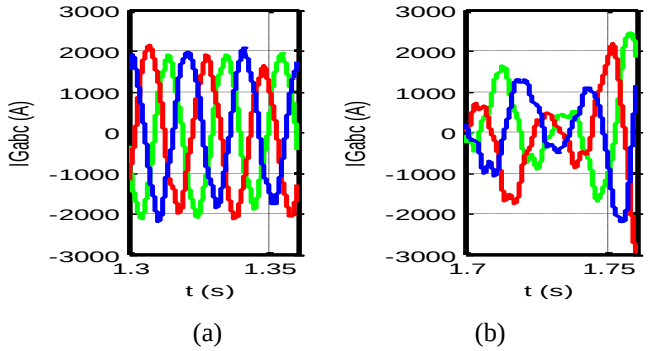

Fig. 6. Waveform of I_{Gabc} currents (a) in healthy and (b) in faulty condition (faulty case F1).

As it can be observed in Fig. 8(c), the rotor faulty phase currents have a harmonic content (red line) with frequences that are odd multiple of *10 Hz.*

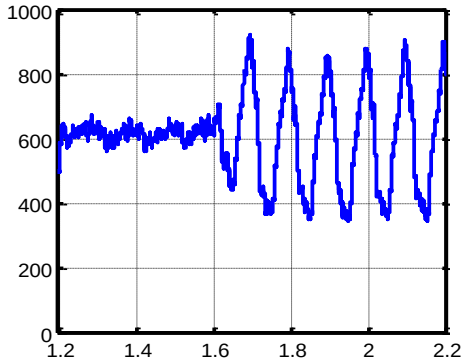

Fig. 7. Waveform of DC link voltage (open circuit occurs in t=1.6sec).

Also a DC component and basic harmonic with lower amplitude (half of the corresponding of the healthy phase-blue line) appear (harmonics with amplitude lower than 2% are not considered measureable). These could be used as a criterion of identification of this fault by measuring only the rotor phase currents. Moreover, it is observed that if this kind of fault happens in the RSC, odd order harmonics occur in the rotor phase currents. On the contrary, when this fault happens in the GSC, even order harmonics occur in the rotor phase currents. Also, in Fig. 9 the rotor voltages in healthy and faulty conditon could be seen.

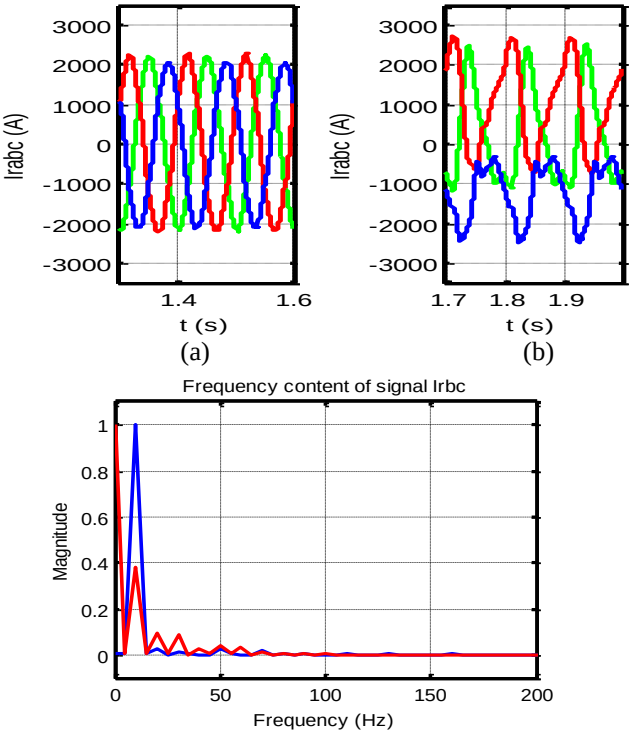

Fig. 8. Waveform of rotor currents (a) in healthy condition, (b) in faulty condition and (c) rotor faulty phase currents' spectrum (blue line-healthy condition, red line-faulty condition).

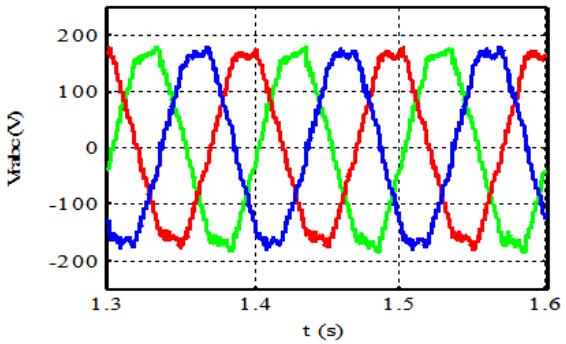

(a)

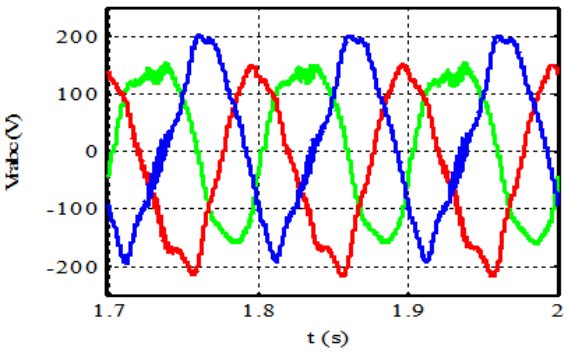

(b)

Fig. 9. Waveform of rotor voltage (a) in healthy (b) in faulty condition

As it is observed in Fig. 10(c), the stator phase currents have a specific harmonic content that is unique for this kind of fault (blue line-healthy condition, red line-faulty condition). Furthermore, this kind of fault (F1) has a high influence on stator's currents and that is very important because these harmonis will be injected to the grid. Also, in

Fig. 11 the waveform of electromagnetic torgue (open circuit fault occurs at t=1.6sec, case F1) and the spectrum of the electromagnetic torque (blue line-healthy condition, red line-faulty condition) is presented. These harmonics are the upcoming because of the corresponding harmonics in stator's currents.

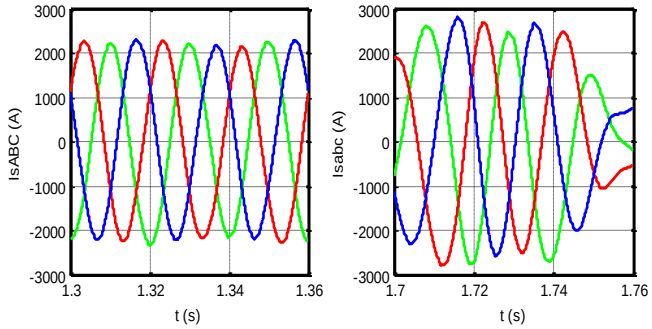

(a) (b)

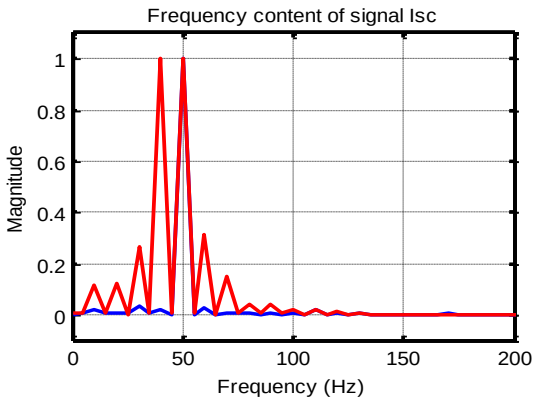

(c)

Fig. 10. Waveform of stator currents in (a) healthy condition, (b) faulty condition and (c) their spectrum.

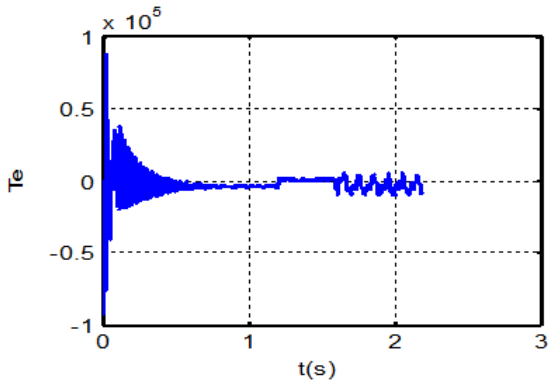

(a)

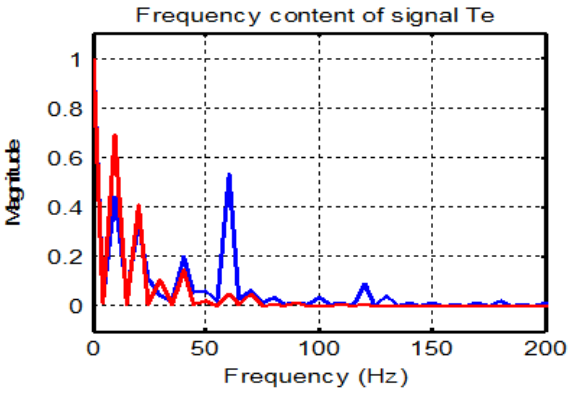

(b)

Fig. 11. Waveform of electromagnetic torgue (open circuit fault occurs at t=1.6sec) and (b) spectrum of the electromagnetic torque (blue line-healthy condition, red line-faulty condition).

5.3. Open-Circuit Faults in GSC

As it is well-known, GSC acts like a boost rectifier in subsynchronous mode. When an open-circuit fault in GSC occurs, its behaviour changes (Fig.3). This may be devastating for the converter. For this reason it is necessary this kind of faults to be immediately diagnosed and cleared from the protection circuits. Simulation results that present

how DFIG reacts, when an open-circuit fault in GSC happens, including the spectrum of some basic system variables are depicted in Figures 12-20.

In Figure 12 the disturbance in case (F2) in the grid phase currents is presented, which is caused by the corresponding disturbance of the Igabc. Also, an increase of these currents' peak value is observed. In Figures 13 and 14 input voltages of the back-to-back converter (V_{gabc}) and phase currents that are fed in the back-to-back converter from the grid (I_{gabc}) are presented. This kind of fault (F2) has a high influence in this part of the system and the distrurbance is obvious.

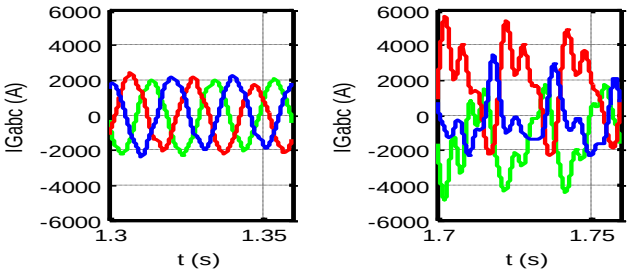

(a) (b)

Fig. 12. Waveform of grid phase currents (a) in healthy and (b) in faulty condition.

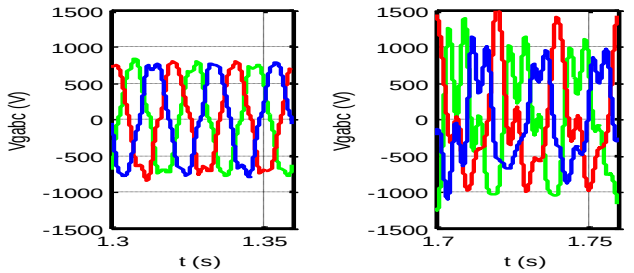

(a) (b)

Fig. 13. Waveform of V_{gabc} voltages in GSC (a) in healthy and (b) in faulty condition.

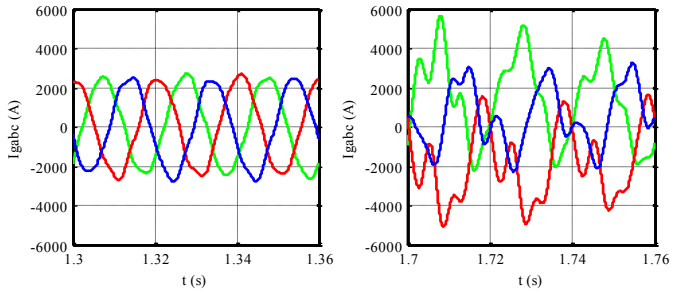

(a) (b)

Fig. 14. Waveform of Igabc currents in GSC (a) in healthy and (b) in faulty condition.

The spectrum of the faulty phase current of GSC (Fig.15) includes a DC component with amplitude comparable to that of the basic harmonic (half of that of the basic harmonic). This maybe lead the inductors to the saturation mode. Also there are 2nd, 3rd, 4th, 5th and 6th harmonics (the higher harmonic can be neglected) in comparison to healthy condition. Harmonics with amplitude lower than 2% are not considered measureable. A range of frequences (*233 Hz-255 Hz*) around of *243 Hz* both in healthy (blue line) condition and in faulty condition (red line) appear. This range of frequences is due to the operation of DFIG (on similar case of fault in a boost rectifier without DFIG this bandwith doesn't appear[14]). In Figure 16 the influence of (F2) in DC link voltage can be seen. The ripple in this case (fault F2) is higher than the corresponding in case of (F1).

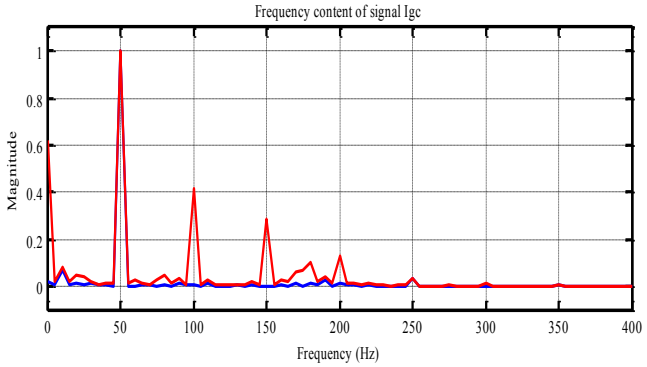

Fig. 15. Spectrum of faulty phase current I_{gbc}.

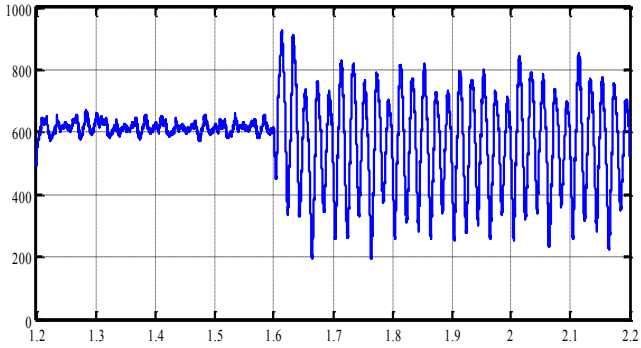

Fig 16. Waveform of DC link voltage (open circuit occurs at t=1.6sec)

In Fig. 17(b) the specrutm of phase rotor current presents harmonics in 10 Hz and even multiples of 10 Hz (harmonics with amplitude lower than 2% are not considered measureable). However, if this kind of fault happens in GSC, the rotor currents are not much affected.

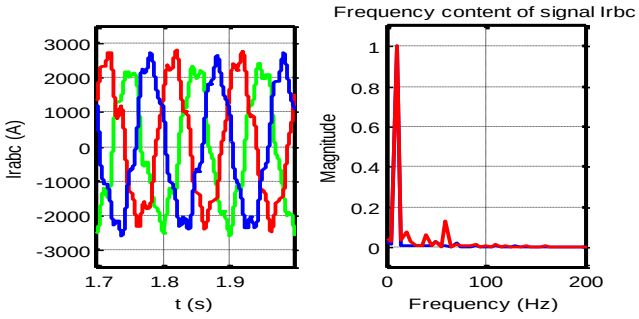

(a) (b)

Fig. 17. Waveform of rotor currents (a) in faulty condition and (b) their spectrum of power density (blue line- healthy condition, red line-faulty condition).

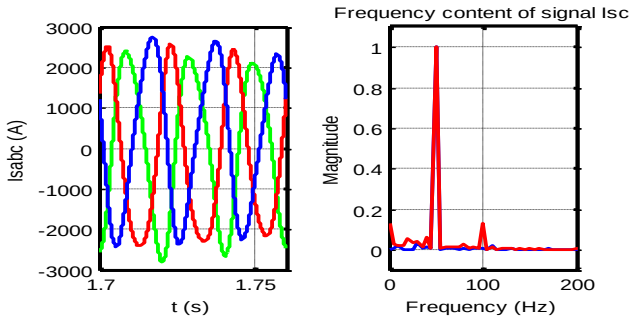

(a) (b)

Fig. 18. Waveform of stator currents (a) in faulty condition and (b) their spectrum of power density (blue line- healthy condition, red line-faulty condition).

In Fig. 19 (b) the spectrum of power density of the electromagnetic torque of the asynchronous machine is shown. Harmonics in *10 Hz, 20 Hz, 50 Hz, 60 Hz, 100 Hz* and a DC component appear (harmonics with amplitude lower than 2% are not considered measureable). This is because the same harmonic occurs in the stator phase current as it is shown in Fig. 18b. As it is well known the interaction between rotor Magnetomotive Force (MMF)'s harmonics and stator's currents harmonics causes harmonics in the electro-magnetic torque respectively [13]. Also, in Fig. 20 the rotor voltages could be seen.

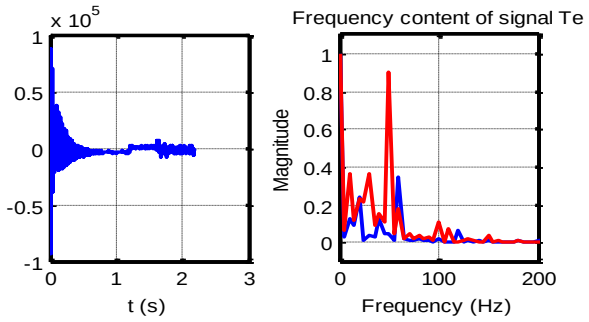

(a) (b)

Fig. 19. Waveform of electromagnetic torgue (open circuit occurs at t=1.6sec) and (b)electromagnetic torque's spectrum (blue line-healthy condition, red line-faulty condition) in the case (F2).

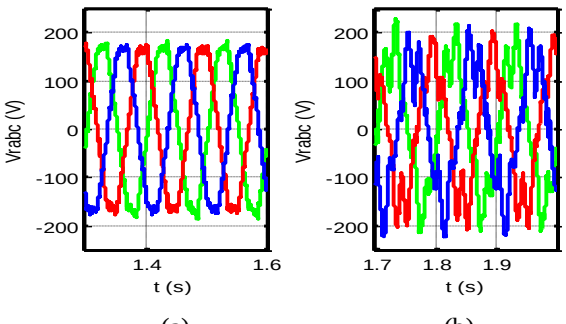

(a) (b)

Fig. 20. Waveform of rotor voltages (a) in healthy and (b) in fault condition in the case (F2).

6. Conclusion

In this work open-circuit faults in the back-to-back converter of a DFIG under the restriction of a constant speed are investigated via simulation in the environment of Matlab/Simulink in order to emerge the consequences of those faults in the operation of DFIG and the need of development of a diagnostic method. Two kinds of open-circuit faults that are possible to happen, an open circuit of two IGBTs in different legs of a converter and an open circuit of one IGBT and one diode, are investigated. These kinds of fault in the RSC and in the GSC respectively with devastating consequences for the whole system are investigated. Observing the spectrums of power density of the basic variables of the system-phase rotor and stator currents and phase currents of the GSC, it is concluded that harmonics occur with specific frequencies. More specifically, when an open-circuit fault in one IGBT and one diode in different legs in GSC happens, a specific harmonic content in GSC's filter input phase currents occurs-odd multiple of 10 Hz and also a DC component and basic harmonic with lower amplitude (half of the corresponding of the healthy phase) appear. This harmonic content is unique for this kind of fault. The part of the system that consists of the RSC and the asynchronous generator is not influenced by this fault. When two IGBTs in different legs are open-circuited in RSC, a specific and unique harmonic content in rotor phase currents, a dc component and 2^{nd}, 3^{rd}, 4^{th}, 5^{th} and 6^{th} harmonics in comparison to healthy condition is observed. These evidences could be used as a criterion on developing a method for fault diagnosis and identification. Indeed, by measuring the phase rotor currents and the GSC's input currents regularly and comparing their spectrum of power density with the corresponding in healthy condition, can conclude, if an open-circuit fault has happened in the back-to-back converter and additionally which is the kind of this fault.

References

[1] R. Pena, J. C. Clare, and G. M. Asher, "Doubly fed induction generator using back-to-back PWM converters and its application to variable-speed wind-energy generation," IEE Proc. Electr. Power Appl., vol. 143, pp. 231-241, May 1996.

[2] D. G. Giaourakis, A. Safacas, "Review of Wind Energy Conversion Systems for Large Wind Turbines and Simulation of a back-to-back Electronic Power Converter", Ever2011, Monte Carlo, Monaco, 31 March-3 April 2011, conference proceedings.

[3] Ned Mohan, Ted K. A. Brekken, "Control of a Doubly Fed Induction Wind Generator Under Unbalanced Grid Voltage Conditions", IEEE Transaction Energy conversion, vol.no22. 1, march 2007 page 129-135.

[4] H. Polinder and J. Morren, "Developments in wind turbine generator systems", Electrimacs 2005, Hammamet, Tunisia, conference proceedings.

[5] Muller S, Deicke M., Rik W., Doncker D.: "Doubly fed induction generator systems for wind turbines", IEEE

Trans Inds. Appl., Magazine 8 (3) (May/June 2002), pp. 26-33.

[6] Ribrant J., Bertling L., "Survey of failures in wind power systems with focus on Swedish wind power plants during 1997-2005", Power Engineering Society General Meeting, 2007. IEEE , pp 1-8.

[7] D. Kastha, B.K. Bose, "Investigation of Fault Modes of Voltage-Fed Inverter System for Induction Motor Drive," IEEE Trans. Ind. Applic.,vol. 30, no. 4, pp. 1028-1037, 1994.

[8] R. L. A. Ribeiro, C. B. Jacobina, E. R. C. da Silva, A. M. N. Lima, "Fault detection of open-switch damage in voltage-fed PWM motor drive systems, " IEEE Trans. Power Electron., vol.18, no.2, pp.587-593, March 2003.

[9] Olimpo Anaya-Lara, Nic Jenkins, Janaka Ekanayake, Phill Cartwrigtht, Mike Hughes, "Wind Energy Generation:Modeling and Control", ISBN 978-0-470-71433-1, John Wiley&Sons, Ltd, 2009.

[10] Tao Sun, "Power Quality of Grid-Connected Wind Turbines with DFIG and Their Interaction with the Grid", Dissertation submitted to the Faculty of Engineering & Science at Aalborg University in partial fulfilment of the requirements for the degree of Doctor of Philosophy in Electrical Engineering Institute of Energy Technology Aalborg University, Denmark, May 2004.

[11] H. Polinder, F.F.A. van der Pijl, G.J. de Vilder, P. Tavner, "Comparison of direct-drive and geared generator concepts for wind turbines", Proc. of the international conference on electrical machines and drives, St. Antonio, 2005.

[12] D. Kastha, B.K. Bose, "Investigation of Fault Modes of Voltage-Fed Inverter System for Induction Motor Drive," IEEE Trans. Ind. Applic., vol. 30, no. 4, pp. 1028-1037, 1994.

[13] R. Peuget, S.Courtine, J.P. Rognon, "Fault Detection and Isolation on a PWM Inverter by Knowledge-Based Model", IEEE Trans. Ind. Applicat., vol. 34, No. 6, pp. 1318-1325, 1998.

[14] M. Trabelsi, M. Boussak, M. Gossa, "Open circuit faults diagnosis of PWM inverter-fed induction motor by stator current signature analysis", 10th International Conference on Sciences and Techniquesnof Automatic Control & Computer Engineering, pp. 1-12 Hammamet, Tunisia, Dec. 2009, Cd-Rom.

[15] Francisco K. A. Lima, Alvaro Luna, Pedro Rodriguez, Edson H. Watanabe, and Frede Blaabjerg, "Rotor Voltage Dynamics in the Doubly Fed Induction Generator During Grid Faults", Ieee Transactions On Power Electronics, Vol. 25, No. 1, January 2010.

[16] Lingling Fan, Subbaraya Yuvarajan and Rajesh Kavasseri, "Harmonic Analysis of a DFIG for Wind Energy Conversion System", Ieee Transactions On Energy Conversion, Vol. 25, No. 1, March 2010.

[17] Lingling Fan, Zhixin Miao, Subbaraya Yuvarajan and Rajesh Kavasseri,"Hybrid modeling of DFIGs for wind energy conversion systems", Simulation Modeling Practice and Theory 18 (2010), Elsevier, pp. 1032-1045.

[18] X. H. Wu, S. K. Panda, and J. X. Xu,, "DC Link Voltage and Supply-Side Current Harmonics Minimization of Three Phase PWM Boost Rectifiers Using Frequency Domain Based Repetitive Current Controllers", Ieee Transactions On Power Electronics, Vol. 23, No. 4, July 2008, Pp. 1987-1997.

[19] Hansen A.D., "Generators and Power Electronics for wind turbines", Chapter in "Wind Power in Power systems", John Wiley&Sons, Ltd, pp. 24-70, 2004.

[20] I. Tsoumas, A. Safacas , «On the Use of the Current Space Vector's Angle and Instantaneous Frequency for Fault Diagnosis in Power Electronics Converters: Application in the Subsynchronous Cascade Drive», International Review of Electrical Engineering (I.R.E.E.), vol. 4N.2, March - April 2009, p.p. 174 -183.

[21] I. Colak, E. Kabalci, R. Bayindir and S. Sagiroglu, "The design and analysis of a 5-level cascaded voltage source inverter with low THD", 2nd PowerEng Conference, Lisbon, pp. 575-580, 18-20 March 2009, conference proceedings.

[22] R. Pena, J. C. Clare and G. M. Asher, "A doubly fed induction generator using back-to-back PWM converters supplying an isolated load from a variable speed wind turbine", IEE Proceedings on Electrical Power Applications, vol.143, issue.5, pp.380-387, Sep. 1996.

[23] Jang, J., Y. Kim and D. Lee, "Active and reactive power control of DFIG for wind energy conversion under unbalanced grid voltage", Proc. IEEE Power Electronics and Motion Control Conference, Shanghai, China, Vol: 3, 2006, pp. 1-5.